AO4ELT7 - June 2023 - Avignon

Finally, let's use all the modes - A stable DM fitting avoiding modal truncation

Andreas Obereder[a], Thomas Bertram[b], Carlos Correia[b], Markus Feldt[b], Stefan Raffetseder[c], Julia Shatokhina[c], and Horst Steuer[b]

[a]Industrial Mathematics Institute, University Linz, Austria
[b]Max Planck Institute for Astronomy, Heidelberg, Germany
[c]Johann Radon Institute for Computational and Applied Mathematics, Linz, Austria

ABSTRACT

METIS SCAO uses a wavefront control concept that deploys a 2-stage spatial reconstruction where the wavefront is first reconstructed on an intermediate space we call the virtual DM, and then projected onto the actual control space. This document addresses the projection of the wavefront estimation on the virtual deformable mirror (VDM) onto the control modes developed for METIS (Mid-infrared ELT Imager and Spectrograph). We present a new approach to project onto the control modes using an intermediate regularized projection on the M4 mirror and then convert to modes. This method enables us to utilise all modes for the projection and control in a stable manner, achieving high Strehl ratios for a wide range of conditions without the need for complex parameter tuning.

Keywords: DM projection, Wavefront Control, Adaptive Optics, Regularisation, METIS, SCAO

1. INTRODUCTION

For the instrument METIS, the baseline approach is a 2-step algorithm [1] for wavefront estimation and subsequent mapping onto the chosen control space. This approach offers advantages in both wavefront estimation and handling misregistration, rotation, and the stability of fitting to control modes [3].

It has already been theoretically and computationally demonstrated that wavefront estimation in a basis specifically tailored to the WFS geometry and using proper regularisation has advantages. We now apply the same principles to the so-called projection step, which involves mapping the WF estimation either directly onto the deformable mirror (i.e., calculating desired actuator positions) or onto a set of modes used to control the DM.

The following requirements should be fulfilled by the projection step (fitting step):

Further author information: (Send correspondence to A.O.)
A.O.: E-mail: andreas.obereder@mathconsult.co.at, Telephone: +43-660-1106894
J.S.: Julia Shatokhina, shatohina.julia@gmail.com

- Ultimate goal: **Smooth DM shapes**
- Few (or even no) parameters to optimise
- Independent of the chosen representation of wavefront (modes)
- Optimised for the hardware used, i.e., the layout of the DM actuators

In this paper, we will describe a method that provides these desired properties and present corresponding results. We will compare this novel approach with the standard fitting method and highlight its advantages.

2. DM PROJECTION USING THE M4 INFLUENCE FUNCTIONS

After the wavefront shape is reconstructed, as described in detail in [1, 3], the next step is to compute the optimal actuator commands for the DM.

We assume a basis of 2D bilinear functions $(h_i)_{i=1,\dots,n_c}$ (finite element basis) for the reconstructed wavefront representation. This basis matches the resolution of the pyramid wavefront sensor. The vector $\vec{c}$ of the reconstructed wavefront coefficients is available on the Fried geometry, and the wavefront is given as

$$\Phi(x,y) = \sum_{j=1}^{n_c} c_j h_j(x,y) = H\vec{c}, \tag{1}$$

where H denotes a matrix that contains the discretized bilinear functions h_j in its rows.

To solve the DM fitting equation and derive the actuator commands $\vec{a} = (a_i)_{i=1,\dots,n_a}$ from the reconstruction Φ, we need to solve

$$\Phi_{rec}(x,y) = \sum_{j=1}^{n_c} c_j h_j(x,y) \cong \sum_{j=1}^{n_a} a_j IF_j(x,y) \tag{2}$$

with exact M4 DM influence functions $(IF_j)_{j=1,\dots,n_c}$ and accurate actuator positions. Let F denote a matrix that contains the M4 influence functions $(IF_j)_{j=1,\dots,n_c}$ (same discretization) in its columns. The DM fitting equation can be rewritten as

$$H\vec{c} \cong F\vec{a}. \tag{3}$$

The goal of the DM projection step is to obtain the vector $\vec{a} = (a_i)_{i=1,\dots,n_a}$ for a given $\vec{c}$ and matrix F in a stable way that does not lead to a loss of information on the wavefront.

A least squares solution to the DM fitting equation is

$$\vec{a} = (F^T F)^{-1} F^T H\vec{c} = F^\dagger H\vec{c} = D_F\vec{c}, \tag{4}$$

where $F^\dagger = (F^T F)^{-1} F^T$ is the pseudo-inverse of F, and $D_F := F^\dagger H$ defines a projection matrix from the reconstructed wavefront coefficients $\vec{c}$ to the coefficients $\vec{a}$ with respect to the space of the DM influence functions.

In practice, the straightforward least-squares projection often leads to instabilities, especially when noisy data is used for the reconstruction. This noise can then be propagated by the projection matrix D_F to the actuator coefficients a and may even be amplified. Instead of the least-squares solution, it is recommended to apply a regularized projection:

$$\vec{a} = (F^T F + \alpha_{proj}\Delta^T\Delta)^{-1} F^T H\vec{c} = F^{reg} H\vec{c} = D_F^{reg}\vec{c}, \tag{5}$$

where Δ denotes the discretized Laplacian operator defined on the M4 influence functions (IF_j), and α_{proj} is a regularization parameter.

The usage of Laplace squared regularization can be described as an embedding in the H_2 Sobolev space, approximating the known statistics of the atmosphere using an H_2 half norm [2]. This regularization is very suitable in the projection step because it imposes a requirement that the DM shape follows the atmospheric statistics. Practically, such regularization smooths the solution by damping its high-frequency content depending on its amount.

2.1 Laplace on M4 - derivation of matrix formulation

Instead of deriving the precise Laplace operator defined on the M4 influence functions (which were obtained by a Finite-Element-Simulation), we approximate the Laplace on a grid defined by the M4 actuator positions and use linear FE ansatz functions on this triangular grid. Figure 1 shows the FE mesh obtained using the M4 actuator positions. The mesh is generated using a Delaunay triangulation, and triangles with small angles are removed in a preprocessing step. One can recognise the regular hexagonal shapes inside every DM segment and the spiders between the segments.

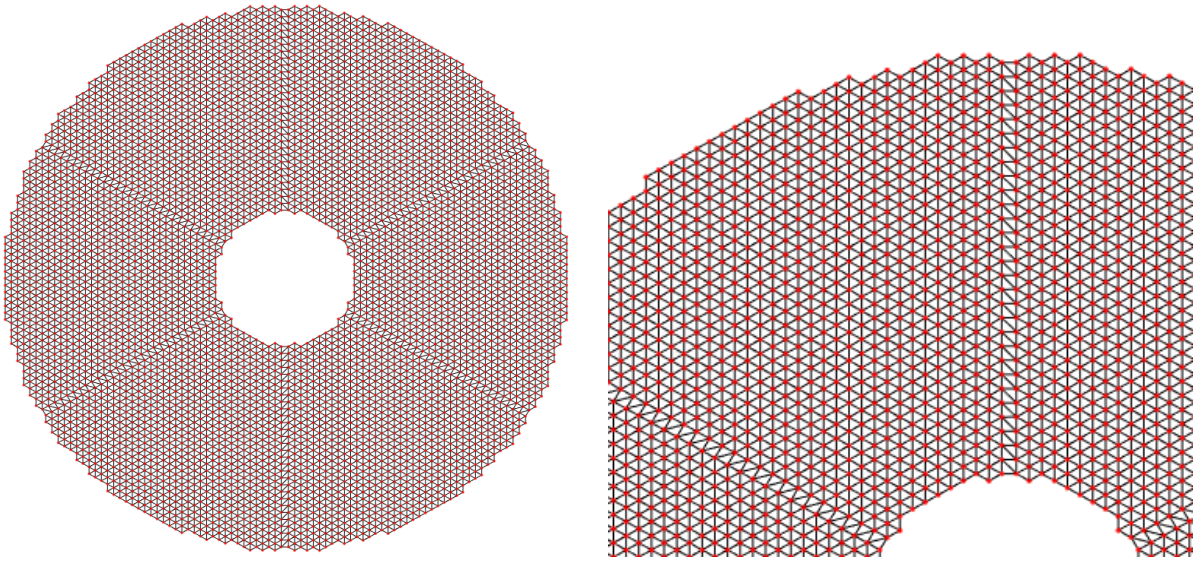

Figure 1. Left: Preprocessed triangular FE mesh defined on the M4 actuator positions. Red: nodes (actuators), black: mesh. Right: Zoomed section of the mesh.

The stiffness matrix of the Poisson equation on this grid now describes the Laplacian used for the projection of the wavefront reconstruction on M4.

3. DM PROJECTION USING MODES

METIS SCAO control relies on a specific set of M4 modes derived to minimize the mechanical load on the DM. The modes-to-command matrix $m2c \in \mathbb{R}^{N_a \times N_m}$ is published to the central control system (CCS*) together with the desired vector $\vec{m}$ of modal coefficients. In our examples, M4 has $N_a = 5352$ actuators, and $N_m = 4303$ modes are used in the control algorithm and for communication with the telescope.

Let M denote a matrix that contains the M4 mechanical modes $(m_j)_{j=1,\dots,N_m}$ as its rows, $M \in \mathbb{R}^{N_m \times N_c}$. Here, the wavefront reconstruction Φ_{rec} is discretized with $N_c = 5602$ ansatz functions on a regular grid.

The DM fitting equation that we want to solve in this case is

$$\Phi_{rec}(x,y) = \sum_{j=1}^{n_c} c_j h_j(x,y) \cong \sum_{j=1}^{n_m} b_j m_j(x,y), \tag{6}$$

or in the matrix-vector-multiplication form

$$H\vec{c} \cong M\vec{b}. \tag{7}$$

The goal is to obtain vector $\vec{b} = (b_i)_{i=1,\dots,n_m}$ for a given $\vec{c}$ and matrix M in a stable way that does not lead to a loss of information about the wavefront.

*CCS controls the adaptive surfaces of the ELT according to the requests made by the instrument.

Similar to Eq.4, the least-squares solution to this problem is given as

$$\vec{b} = (M^T M)^{-1} M^T H \vec{c} = M^\dagger H \vec{c} = D_M \vec{c}, \tag{8}$$

where $M^\dagger = (M^T M)^{-1} M^T$ is the pseudo-inverse of M, and matrix $D_M := M^\dagger H$ defines a projection matrix from the reconstructed wavefront coefficients $\vec{c}$ to the modal coefficients $\vec{m}$ with respect to the modal control space.

As in the reconstruction case above, the straightforward least-squares projection is in practice often related to instabilities, especially for the high-order modes. In this case, for stability reasons one has to truncate the number of controlled modes, which may lead to a loss of the high-frequency information of the wavefront since

$$\tilde{\Phi} = \sum_{j=1}^{N_d < N_m} b_j m_j \neq \Phi. \tag{9}$$

A truncation of modes always leads to a reduction of the approximation quality of the wavefront, see Figure 2 for an example.

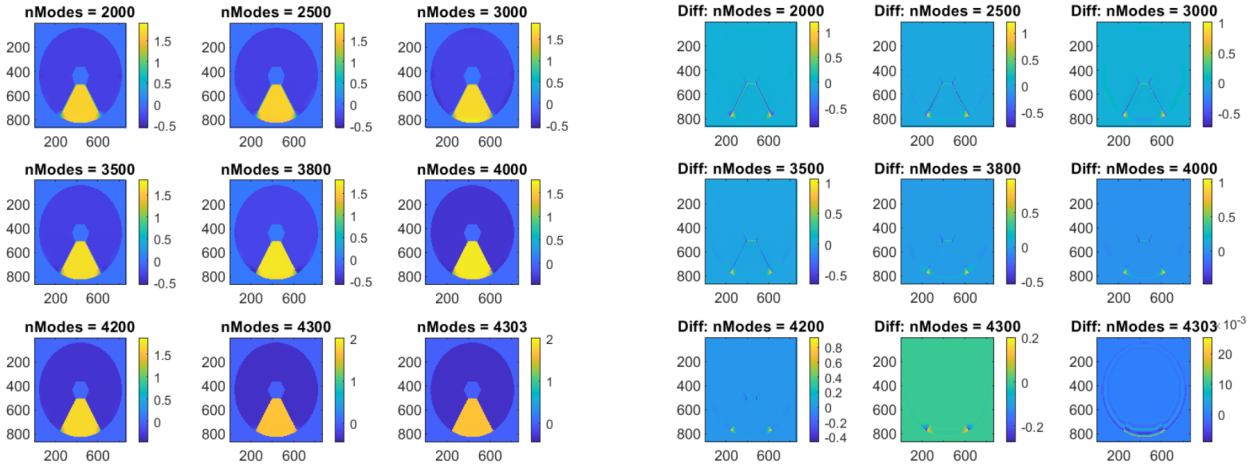

Figure 2. Approximation quality of a segment piston in dependency on the number of used modes. On the left, we see the representation of a segment piston in the truncated modal basis, on the right, the representation error introduced due to truncation.

Instead of a least-squares projection followed by modal truncation, we follow a different two-step approach. Firstly, we project the reconstructed coefficients c to a vector of M4 actuator commands a (in the DM influence functions space) by using the regularized operator D_F^{reg} defined above

$$\vec{a} = D_F^{reg} \vec{c}. \tag{10}$$

Secondly, the M4 actuator commands are projected onto the modal basis. For this, we rely on the available $m2c \in \mathbb{R}^{N_a \times N_m}$ matrix that maps the modal coefficients $\vec{m}$ onto the M4 influence functions space. The pseudo-inverse of it is given by

$$c2m = (m2c^T * m2c)^{-1} m2c^T \tag{11}$$

and it performs the projection in the opposite direction, i.e., from the space of the M4 influence functions to the space spanned by the chosen modal basis,

$$\vec{m} = c2m * \vec{a}. \tag{12}$$

The resulting vector m of modal coefficients covering the complete modal basis is then sent to the controller. The regularization parameter α_{proj} offers a degree of freedom here. Depending on the choice for the level of

regularization α_{proj}, one can vary the amount of frequency-dependent damping. For instance, if the high-frequency content of the solution has moderate amplitudes, a small α_{proj} is chosen for a stable projection. If the high-frequency content of the solution has large amplitudes, one can increase α_{proj} and damp more. Note that very high α_{proj} values would be effectively equivalent to a truncation of the high frequencies and a damping of the lower frequencies.

The method described in (10)-(12) has been implemented in the METIS simulation environment *Compass* and is already used to obtain the results provided in [5] (Sections 7.5.3-7.5.4), whereas the least-squares with truncation was used in other results presented in [5]. The regularized modal projection has several benefits over the standard least-squares projection on a set of truncated modes:

- It provides an improved and more stable performance over the whole range of changing atmospheric conditions (Fried parameter, zenith angle).
- The high performance and stability for a wide range of conditions are achieved with a single fixed value for the regularization parameter. Moreover, projection is done on all elements of the chosen modal basis, and therefore the method is free from the need to optimize the number of modes to be used, which is required for the direct least-squares projection method to make it stable.

4. RESULTS

In this section, we will highlight the properties of the regularized DM projection method, showing its impact on the modal coefficients and the actuator forces of the DM, respectively.

4.1 Playground Example

This pure playground example shows that, in contrast to a pure truncation or damping of the modes, the modal coefficients change globally when the resulting wavefront is smoothed.

For the initial input, we set all modal coefficients equal to one. The impact of utilizing different regularization parameters is shown in Figure 3.

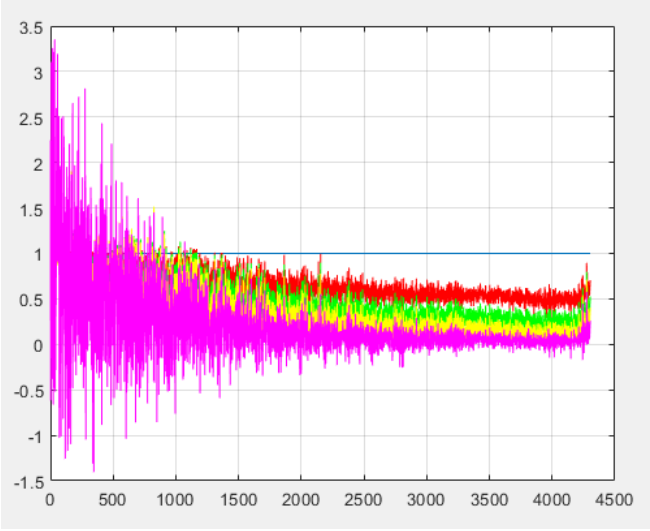

Figure 3. The 4303 modal coefficients for increasing regularization strength.

As expected, the high modal coefficients (high frequencies) are damped. Note that the coefficients of the modes representing low frequencies are changed as well. In order to represent the smoothed wavefront, *all* coefficients are adapted accordingly. Figure 4 emphasizes that with stronger regularization (i.e., smoothing), the modal representation of the wavefront results in a significant adjustment also of the lower modal coefficients.

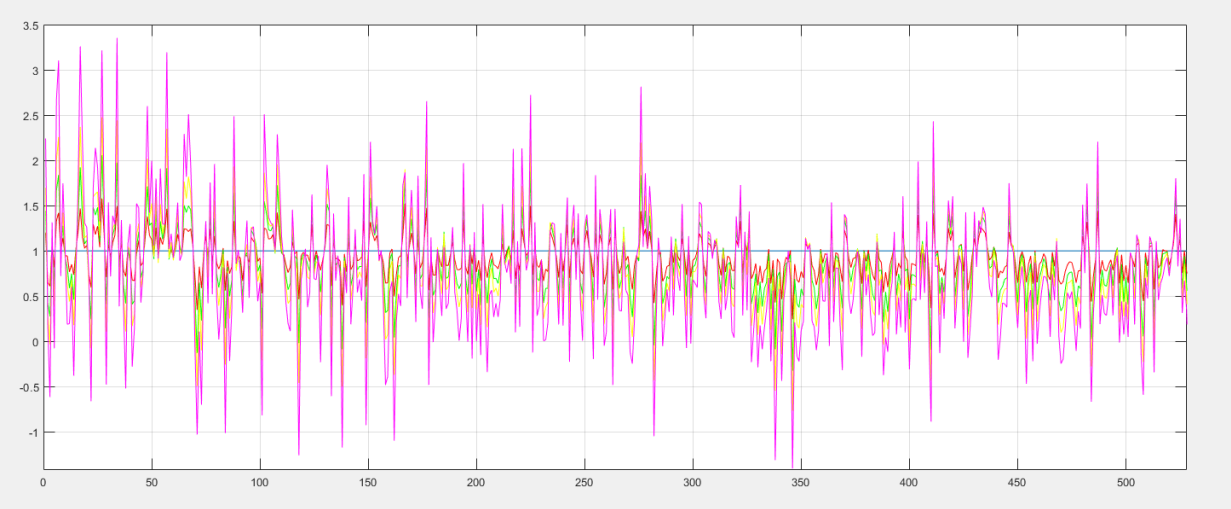

Figure 4. Zoom of the first 500 modal coefficients

4.2 Application on Atmospheric Screens

Our first results visualization compares the old benchmark, namely using a least-squares projection on a reduced number of modes (4000 out of 4302) with the new benchmark, the regularized projection. We compare the modal coefficients obtained for the same input screen using both methods and different regularization parameters ($\alpha_{proj} = 0.01/0.1/1$), see Figure 5.

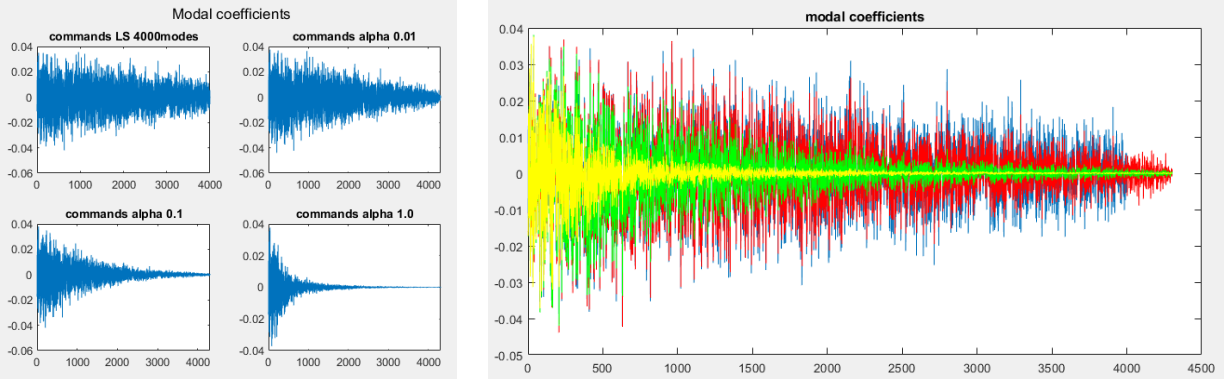

Figure 5. Left: Modal coefficients for different projection algorithms/parameters. Right: Combined plot for better comparability.

One of our main goals was to ensure a smooth (and stable) DM shape. Finally, we present the obtained DM shapes, see Figure 6 and, of crucial importance when controlling a DM, the actuator forces for different regularization parameters, see Figure 7.

5. SUMMARY

By employing direct projection onto the M4 influence functions with the regularization method outlined above, we achieve exceptional and stable performance across various conditions, including atmospheric variations, zenith angles, and guide star brightness levels. When a modal basis is explicitly defined using the M4 influence functions, we recommend using this regularized projection approach via M4 instead of a direct least squares projection onto those modes. This approach enhances both temporal stability and overall quality. Moreover, it enables us to

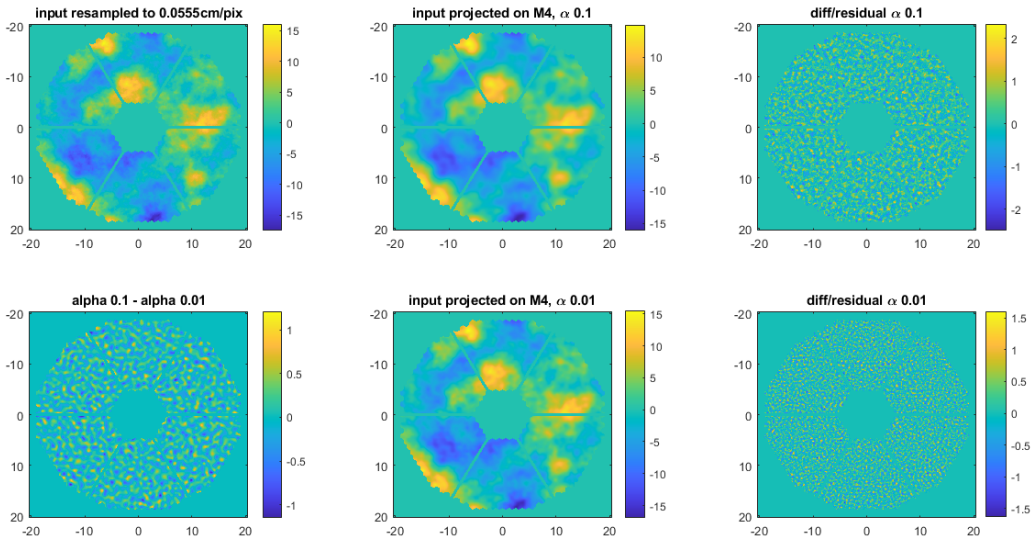

Figure 6. Top Left: atmospheric input screen. Top Mid: projection on DM using $\alpha_{proj} = 0.1$. Top Right: projection residual for $\alpha_{proj} = 0.1$.
Bottom Left: difference between the projections. Bottom Mid: projection on DM using $\alpha_{proj} = 0.01$. Bottom Right: projection residual for $\alpha_{proj} = 0.01$.

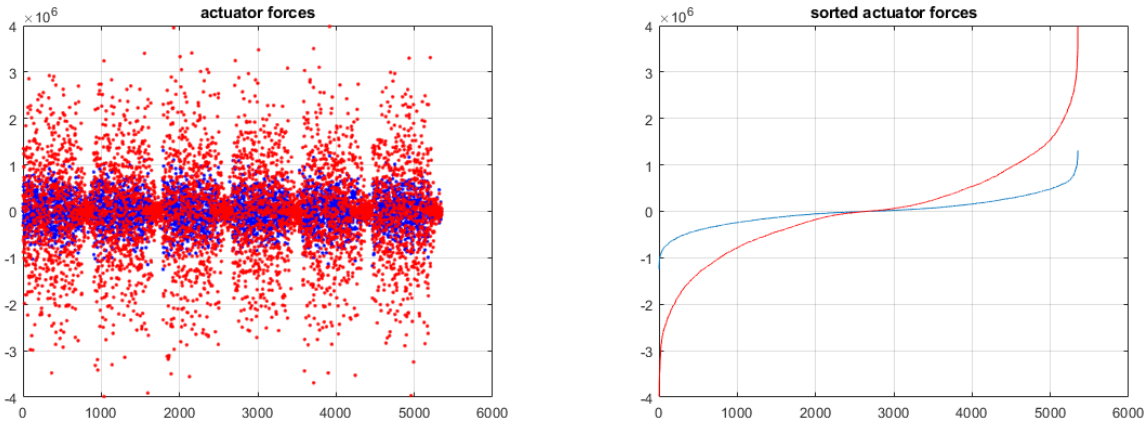

Figure 7. Actuator forces for different regularization strength, red: $\alpha_{proj} = 0.01$, blue: $\alpha_{proj} = 0.1$
Left: actuator forces over actuator numbering. Right: sorted actuator forces.

utilize all available modes without the need for modal truncation to prevent instability during the projection step, thereby preserving high approximation quality. Modal truncation may still occur within the Central Control System (CCS) as part of saturation management; for detailed information, refer to [4] and Section 6.1.4 of [5].

In a practical application, specifically in the simulation of the ELT instrument METIS using the *Compass* framework, our proposed method has consistently demonstrated superior performance. In the context of METIS, it has led to a substantial improvement in wavefront error RMS, with enhancements of up to 60nm. Additionally, there was a noteworthy increase of 1 percentage point in the L-Band Strehl ratio, elevating it from 94.7 to 95.7 under median atmospheric conditions with a zenith angle of 30 degrees.

Another major advantage of this fitting method is its simplicity when selecting the regularization parameter,

α_{proj}. Notably, a fixed value for this parameter consistently delivered outstanding performance across diverse atmospheric conditions, making this projection algorithm readily applicable.

ACKNOWLEDGMENTS

We extend our gratitude to our colleagues and coauthors who have continuously challenged our ideas, thereby contributing to the refinement of our work. Special thanks are owed to Miska Le Louarn and Christophe Verinaud for their ongoing discussions and inspiration in the realm of Adaptive Optics.

This project has received funding from the Austrian Science Fund (FWF) F6805-N36 (Tomography in Astronomy), the Austrian Research Promotion Agency (FFG) No. FO999888133 (Industrial methods for Adaptive Optics control systems), and the NVIDIA Corporation Academic Hardware Grant Program.

References

[1] *Baseline algorithm for wavefront reconstruction for METIS SCAO*. E-TNT-AST-MET-1004. Version 2.0. Apr. 9, 2021. URL: https://polarion.astron.nl/polarion/redirect/project/METIS/workitem?id=METIS-7742.

[2] Simon Hubmer, Ekaterina Sherina, and Ronny Ramlau. "Characterizations of adjoint Sobolev embedding operators with applications in inverse problems". In: *Electron. Trans. Numer. Anal.* 59 (2023), pp. 116–144. DOI: 10.1553/etna_vol59s116.

[3] *Improved implementation of the METIS baseline wavefront reconstructor and M4 projection in COMPASS*. E-TRE-AST-MET-1011. Version 1. URL: https://tc.astron.nl:3000/#/com.siemens.splm.clientfx.tcui.xrt.showObject?uid=QjAAQVICYbaBBD.

[4] *METIS SCAO Wavefront Control Strategy*. E-REP-MPIA-MET-1137. Version 1.

[5] *SCAO Performance Analysis Report*. E-ANR-MPIA-MET-1033. Version 2.

[6] Iuliia Shatokhina, Victoria Hutterer, and Ronny Ramlau. "Review on methods for wavefront reconstruction from pyramid wavefront sensor data". In: *Journal of Astronomical Telescopes, Instruments, and Systems* 6.1 (2020), pp. 1–39. DOI: 10.1117/1.JATIS.6.1.010901. URL: https://doi.org/10.1117/1.JATIS.6.1.010901.